Thermophotovoltaics (TPVs), solar and wind assisted hydrogen production and utilisation in iron and steel industry for low carbon emissions.

Linus Onwuemezie, Hamidreza Gohari Darabkhani* h.g.darabkhani@staffs.ac.uk

Department of Engineering, School of Digital, Technologies and Arts (DTA), Staffordshire University, Stoke-on-Trent, ST4 2DE, UK

HIGHLIGHTS

- H_2O electrolysis powered by solar, wind and thermophotovoltaic were studied.
- CO_2-free from oxy-hydrogen firing ovens and furnaces.
- Recovered heat for H_2O distillation and steam production for PEMEC and WGS units.
- O_2 from the electrolyser cells as one of the feedstocks for the BF and BOF.
- 1002kg/hr of CO_2 by-product from every 626kg/hr of steel was captured.

GRAPHICAL ABSTRACT

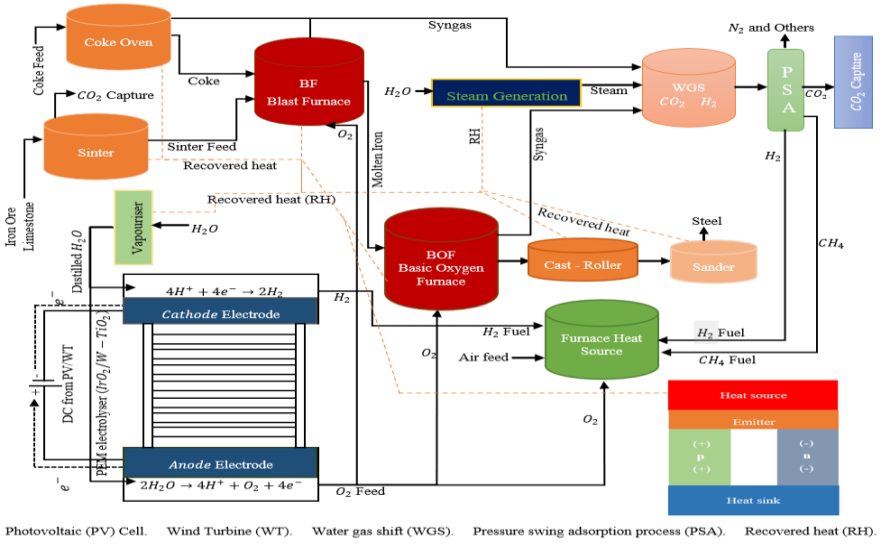

Abstract

To reduce greenhouse gas (GHG) emissions in high-grade steel production plants, this study developed a solar and wind assisted H_2-fuelled blast furnace – basic oxygen furnace (BF-BOF) route coupled with the electrolysis of H_2O and thermoelectric units. The developed model consists of heat recovery units, water gas shift (WGS), low-temperature electrolysis of H_2O, thermophotovoltaic converter, CO_2 capture by absorption and oxy-hydrogen firing ovens and furnaces. The recovered thermal energy generated steam and distilled H_2O feedstocks for WGS and PEMEC (proton exchange membrane electrolyser cell) units. WGS converted CO to CO_2 and increased the H_2 production rate before separation from other by-products in the pressure swing adsorption (PSA) column. H_2O electrolysis generated more H_2 fuel for the coke oven, Fe-CaO oven-sinter, BF and BOF. The result of the proposed system reveals that by utilising H_2 as fuel and O_2 as oxidant instead of burning natural gas (NG) for thermal decomposition of feedstocks, 1111.4kg/hr of CO_2 emission for every 626kg/hr of produced steel can be prevented. The application of CO_2 capture by absorption process eliminated CO_2 emission footprint from the process. Whereas 61.1kW was recovered by installing TPV units on ovens and furnaces' walls for conversion of waste heat to electricity. By incorporating either solar or wind renewable energy systems with a power output of 20MW, 1290.4kg/hr of H_2 fuel and 38.5kg/hr of CH_4 were stored for later use and 6754.8kg/hr of CO_2 emission was avoided. The steel purchase price of the proposed system is anticipated to be cheaper than the conventional BF-BOF route operating with a CCS unit as ≥10% energy efficiency was recorded. The recycling of more scrap steel is also viable in this developed system because of the high energy density of utilised H_2 fuel for the thermal decomposition of ovens and furnaces' feeds.

Keywords:
H_2 fuelled blast and basic oxygen furnaces; Blue-green H_2 and O_2 production; Solar and wind renewable energy sources; Thermoelectric converter system; low-temperature H_2O electrolysis; Green steel production.

Nomenclature

Abbreviations and Symbols

AEC	Alkaline electrolysis cell
ASU	Air separation unit
BF	Blast furnace
BOF	Basic oxygen furnace
COG	Coke oven gas
CCS	Carbon capture and storage
DRI	Direct reduction of iron
EAF	Electric arc furnace
GHG	Greenhouse gas
HTF	Heat transfer fluids
HTS	High-temperature shift
HX	Heat exchangers
kg/hr	Kilo gram per hour
$kmol/hr$	Kilo mole per hour
kW	Kilowatt
LTS	Low-temperature shift
MJ	Megajoule
MMBtu	Metric Million British Thermal Unit
MOE	Molten oxide electrolysis
MW	Megawatt
NO	Nitric oxide
NOx	Nitrogen oxides
NREL	National renewable energy laboratory
PEMEC	Proton exchange membrane electrolyser cell
PSA	Pressure swing adsorption
PV	Photovoltaic
SAM	System Advisor Model
SMR	Steam methane reforming
SOEC	Solid oxide electrolysis cell
TPVs	Thermophotovoltaics
WGS	Water gas shift
WT	Wind turbine

1. Introduction

Nowadays, the reduction of greenhouse gas (GHG) emissions has attracted global attention because of climate change and the repletion of energy resources. The iron and steel industries account for 7% of worldwide carbon dioxide (CO_2) emissions which release about 2 tonnes of $CO_2/tonne$ of produced steel [1]. The global production of steel is predicted to reach 2.19 billion tonnes and recycling of scrap steel through electric arc furnace (EAF) is likewise projected to account for 50% by 2050 [2] [3]. The reduction of carbon emissions in steel and iron production plants can be achieved by the introduction of waste energy recovery, switching to renewable energy sources and low carbon fuels and efficiency improvement. For instance, the recovery of waste energy in a process and utilising it to operate other units can reduce the overall input energy and the volume of carbon emissions which is beneficial to the environment [4]. While approximately 60% of the total energy used in steel production is lost to cooling which may be recovered and utilised for different purposes [5]. Currently, blast furnace-basic oxygen furnace (BF-BOF), electric arc furnace (EAF) and direct reduction of iron (DRI) are the three major routes for making steel [6].

The blast furnace-basic oxygen furnace (BF-BOF) pathway of making steel includes the iron ore reduction in the blast to produce molten iron and accounts for 70% of worldwide steel production [7] [8]. This route of making steel through integrated BF-BOF requires coal for coke production in the coke (carbon) oven, iron ore (Fe_2O_3 and Fe_3O_4) pelletising to aid BF operation and limestone ($CaCO_3$) for extracting lime (CaO) raw material. The process of producing molten iron and steel includes thermal decomposition of coal, Fe_2O_3 and $CaCO_3$, sintering where reduced Fe_2O_3 mix with CaO in the sinter and blast furnace (BF) where coke and sinter by-products are cooked at about 1000°C temperature. Followed by the introduction of pressurised pure oxygen (O_2) and coolant (scrap steel "20 - 25%") in the basic oxygen furnace (BOF) to produce molten steel. The final steps of producing the finished product (steel) involve casting, rolling, and cooling [9]. Despite the usage of recovered syngas from the coke oven and water gas shift (WGS) units as part of the furnace's fuel, between 2140 and 2227kgCO_2/tons crude steel is produced from this process (BF-BOF) [10]. For instance, BF accounts for 69% of CO_2 emission, 5% for coke production, 13% for sintering, 2% for pelletising and 11% for BOF in the BF-BOF route of steel making [10]. To reduce the volume of CO_2 emission in BF-BOF steel plants, the use of coke from biomass wood and the burning of biogas such as hydrogen (H_2) has been suggested. The replacement of coke from coal with biomass such as charcoal has been studied extensively [11] [12]. These charcoal substitution studies suggested blending 2% – 6% with coking coal, 0% – 100% with pulverised coal, 50% – 100% with nut coke and 0% - 100% with coking plant residues [13]. However, the high cost and porosity of biomass based-charcoal slow down such transition of using coke from charcoal in the BF. For example, coal is denser, and the porosity is 3 times lesser than coke from biomass such as charcoal [13]. As reported by *Geerdes et al.*, a BF coke should have a low sulphur content, hardness, alkali (H_2O and Na_2O) content, moisture, ash and high heating value (HHV) properties for good grinding and to prevent refractory lining and sticking [14]. Burning of low-carbon fuel like biofuel or H_2 has been an area of interest to reduce the size of carbon capture and storage (CCS) units for steel and iron plants. For instance, by replacing the burning of fossil fuels with biohydrogen fuel, >80% of CO_2 emission can be avoided [15]. In addition, *Arens et al.* mentioned that the use of H_2 fuel for operating the BF, and electricity as an energy source for

the EAF in an integrated steel-making plant can achieve zero carbon emissions [16]. Although, the European Commission's carbon reduction target (80%) in the iron and steel-making industry can be achieved by H_2 direct reduction and the electrolysis of iron ore [17].

An electric arc furnace (EAF) is regarded as the best route for using scrap steel (recycling) as feedstock in making brand-new steel. Unlike hybrid BF-BOF pathways of producing steel, EAF uses both electrical and chemical energy to melt the feedstock which is a mixture of scrap metal and carbon sources like coal, coke, and petrol. The introduction of chemical energy requires oxyfuel burners or scrap contaminants that contain hydrocarbons like paints, oil, grease and charged carbon [18]. The global share of the EAF route is growing with over 18143.7 million tonnes of steel production as of 2018. Currently, the share of EAF in steel production is over 24% because of the flexibility of accommodating mixed feedstocks. Despite the use of recycled steel and continuous growth of the EAF, about 40% of natural gas and coal, and between 5958 and 8806kWh/t of electrical energy are consumed in this process resulting to $2.6tCO_2/t_{steel}$ emission [19]. In contrast to the BF-BOF route of steel production, EAF CO_2 emission is approximately 20% lower. This figure shows that an increase in steel production from EAF remains the alternative means of reducing carbon emissions and energy demand. However, limitations in the feedstock (scrap steel) supply, the use of grid electricity resulting in power quality issues and low market share for applications that require higher grade steel limit the widespread of this route in global steel production [20] [4]. Nevertheless, off-grid electricity generation by renewable sources like wind and solar has been suggested to mitigate one of the drawbacks.

The direct reduction of iron (DRI) allows the use of synthetic gas from hydrocarbons or solid fuels enriched in carbon monoxide (CO) and H_2 as the reducing agent to reduce iron ore below the melting point (1200°C). This route of making both sponge and briquette irons is more energy efficient with lesser CO_2 emission than other processes [21]. However, it requires the integration to another route such as EAF for upgrade or additional processing. As of 2020, the global steel production by DRI route reaches 104.4Mt with gas-based accounting for 75.6% [22]. On the contrary, the presence of sulphur content and the inability to produce high-grade steel through gas-based shaft furnaces limit the growth of this route in a single unit [22]. Electrolysis of iron ore such as molten oxide electrolysis (MOE) has been suggested as the way forward in reducing the carbon footprints on existing steel-making processes. For over 100 years, the MOE route of making tonnage metal – aluminium, lithium, magnesium, sodium, and rare-earth metals has been existing because the process produces O_2 and free CO and CO_2. Despite reduced plant size by utilising a single unit for steel production, the use of electricity as an energy source and reduced CO_2 emission, the MOE pathway of steel making is energy intensive. For example, a reaction temperature of 1600°C is needed to dissolve iron ore in a molten oxide mixture [23]. The chemical reactions of the Fe-CaO oven and coke oven under thermal conditions are represented in Eqs 1 – 3. While chemical reactions of both Fe_2O_3 and Fe_3O_4 reduction by synthetic gas are written in Eqs 4 – 9.

$$Fe_3O_4 + CaCO_3 \rightarrow 3Fe + 2O_2 + CaO + CO_2 \quad (1)$$

$$Fe_2O_3 + CaCO_3 \rightarrow 2Fe + 1.5O_2 + CaO + CO_2 \quad (2)$$

$$Coal \rightarrow Coke + gas\ (H_2, CO, CO_2, N_2\ and\ O_2) + H_2O \quad (3)$$

$$3Fe_2O_3 + H_2 \rightarrow 2Fe_3O_4 + H_2O \quad (4)$$

$$Fe_3O_4 + H_2 \rightarrow 3FeO + H_2O \quad (5)$$

$$FeO + H_2 \rightarrow Fe + H_2O \quad (6)$$

$$3Fe_2O_3 + CO \rightarrow 2Fe_3O_4 + CO_2 \quad (7)$$

$$Fe_3O_4 + CO \rightarrow 3FeO + CO_2 \quad (8)$$

$$FeO + CO \rightarrow Fe + CO_2 \quad (9)$$

To sum up, the above-reviewed articles cover different steel production routes such as BF-BOF, EAF, DRI and MOE; the use of renewable feedstocks like coke from biomass charcoal as a substitute for coke from coal. Most of the high-grade steel is produced from BF-BOF. However, the carbon emissions share of this route (BF-BOF) is higher than other routes. Recycling more scrap steel and the use of electricity by DRI-EAF make it more attractive than BF-BOF. Nonetheless, the DRI-EAF route is limited to applications that require higher-strength steel and still has carbon footprints. MOE on the other hand is still in the development phase and the carbon emission footprints can only be determined by the sources of electrical energy. Replacing coke from coal with biomass coke can reduce the overall carbon footprint. Nevertheless, biomass coke such as charcoal is more expensive and still has carbon footprints if fossil fuel is burnt in the pyrolysis decomposer to produce carbon and synthetic gas. Other ways to reduce carbon

emission footprints are the burning of low carbon fuel like H_2 gas in the furnaces and the use of renewable energy sources such as solar, wind, geothermal and others to generate required electricity. In contrast, H_2 production from fossil fuels is cheaper and emits carbon emissions. Thus, the future of iron and steel making requires the application of more energy recovery units, the use of low-carbon fuel and renewable energy generated at the site of operation such as the electrolysis of H_2O powered by solar and wind power sources.

The electrolysis of H_2O generates H_2 and O_2 as by-products by the electrochemical splitting of H_2O feedstock. In H_2O electrolysis of H_2 production, direct current (DC) from renewable energy sources like solar, wind and biomass can be used to exclude carbon emissions from the process. Alkaline electrolysis cell (AEC), solid oxide electrolysis cell (SOEC) and proton exchange membrane electrolysis cell (PEMEC) are the three main types of electrolysis of H_2O technologies. Each of these technologies for H_2 production utilises different operating temperatures, electrolytes, and ionic agents (OH^-, H^+, O^{2-}). For example, AEC and PEMEC have an operating temperature below 100°C and use potassium hydroxide (KOH) or sodium hydroxide (NaOH) electrolytes. While SOEC uses an intermediate temperature between 500°C and 1000°C [24]. The larger current density, response time, compactness, and low operating temperature of PEMEC make it more suitable for industrial applications [25] [26]. DRI-EAF steel production route operating with low-carbon fuel like green H_2 from the electrolysis of H_2O and powered by renewable energy sources has been projected to be more cost-effective in regions with higher solar intensity and wind speed than other routes. Between 2020 and 2021, an increase from $547/t to $782/t of steel sales price in a selected site was reported because of surges in feedstock and fuel prices, making H_2-based DRI-EAF more economically practical. Iron and steel making via H_2-fuelled DRI-EAF has been forecasted to reach 60% share of global steel production by 2050 as the alternative means of reducing GHG emissions in conventional DRI-EAF [27]. Eqs 10 – 12 are chemical reactions of H_2 conducting PEMEC.

$$\text{Anode: } 2H_2O \rightarrow 4H^+ + O_2 + 4e^- \quad (10)$$

$$\text{Cathode: } 4H^+ + 4e^- \rightarrow 2H_2 \quad (11)$$

$$\text{Overall: } 2H_2O \rightarrow 2H_2 + O_2 \quad (12)$$

Another means of maximising energy efficiency in iron and steel-making plants is the integration of thermophotovoltaics (TPVs). As reported by *BCS.* [28], about 20% - 50% of energy in thermal applications ends up in the environment without appropriate recycling strategies. Due to the complex nature of the iron and steel manufacturing industry, waste heat recovery from coke and iron ovens, BF, BOF and molten steel cooling can play an important role in decarbonising the iron and steel industry. TPV utilises heat or waste heat to energise the emitter, and in the process, electricity is generated through the thermocouple effect between the electron donor and acceptor materials [29]. The TPV method of electricity generation has an efficiency between 10% and 40%, depending on the temperature of the heat source. For example, using traditional thermoelectric materials, a maximum efficiency of 10% can be achieved. By using new thermoelectric materials at higher emitting temperatures, 40% efficiency can be achieved [30].

Currently, more effort is channelled to the reduction of carbon emissions in DRI-EAF by the usage of H_2 fuel, solar and wind energy sources despite that this route is limited to producing higher grade steels. In this study, solar or wind oxy-hydrogen firing BF-BOF, coupled with CO_2 capture by absorption method was studied. The application of thermoelectric units for energy recovery and steam production from molten steel cooling was also investigated. This study also includes the diversion of coke oven and furnace (BF and BOF) syngas to water gas shift (WGS) units to produce H_2 fuel with the addition of steam. The production of distilled H_2O feedstock for the PEMEC by syngas cooling in the heat exchanger (HX) was examined. Furthermore, the use of H_2 fuel from PEMEC and PSA units as fuel for the coke oven, Fe-CaO oven-sinter, BF and BOF was covered. Oxy-firing instead of air-firing in any of the thermal units and the usage of produced O_2 from the PEMEC as BF and BOF feedstock was also assessed. This approach eliminates the need for pure O_2 production from air separation unit (ASU) which increases the operational cost and reduces carbon emission footprints without affecting the overall efficiency. This study aimed to apply the stated approaches to enhance energy recovery efficiency and enable the production and usage of biohydrogen fuel in high-grade steel-making plants (BF-BOF). High-grade steels are steels with high strength, quality and toughness at −60°C, and excellent ductility. These steels (high-quality steels) are mainly used in pipelines, reactors, naval vessels and blast (explosive) test designs due to their high resistance to deformation and fracture [31]. The proposed work covers the below points in a process simulation:

1. Process simulation of molten iron production in the BF using coke from oven and sinter by-products and molten steel production in the BOF.

2. Application of WGS to convert syngas from coke oven, BF and BOF into H_2 gas and recovery of methane (CH_4) gas from other by-products.
3. Application of heat recovery units to produce steam for WGS and deionised H_2O for electrolysis stack and electricity via thermophotovoltaic converters.
4. Application of PEMEC using produced deionised H_2O feedstock for H_2 and O_2 production and O_2 feed to both furnaces.
5. Integration of both solar and wind renewable energy sources to power electrolyser stack and other electrical units.
6. By-product CO_2 capture by absorption method.
7. Numerical investigation of steam production from hot-rolled molten steel.
8. Oxy-hydrogen firing burner for thermal decomposition of coke oven, Fe-CaO oven-sinter, BF and BOF feeds.

Fig. 1 displays a schematic diagram of solar and wind assisted oxy-hydrogen firing BF-BOF, PEMEC and thermoelectric converter, coupled with by-product CO_2 capture.

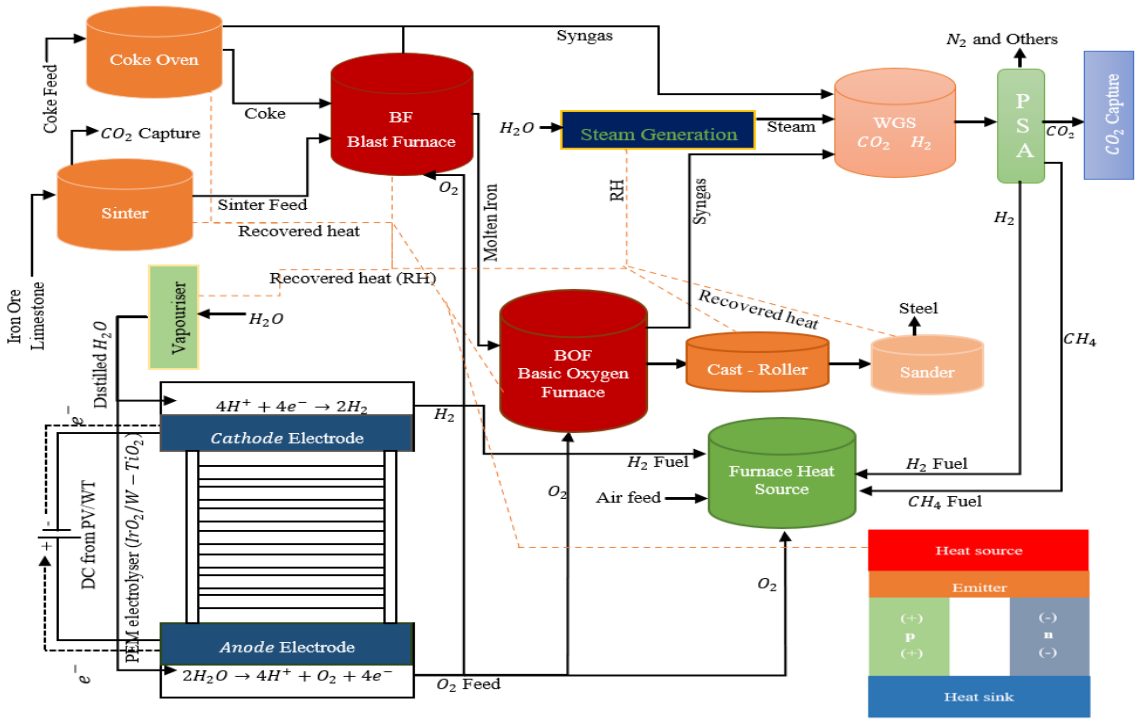

Fig 1: Solar and wind assisted oxy-hydrogen firing BF-BOF, PEMEC, thermoelectric converter and CO_2 capture.

2. Material and simulation method

Feedstock includes 5kmol/hr of iron ore (hematite (Fe_2O_3)) with output gas composition of 10% silicon (Si), magnesium (Mg), sulphur (S), phosphorous (P) and others; 5kmol/hr of limestone ($CaCO_3$); and 20kmol/hr of coal containing 40% of coke (carbon), 57% of gas and 3% of others (ash or slag). 2.4kmol/hr of CH_4, 1.8kmol/hr of H_2O, 0.768kmol/hr of CO, 5.76kmol/hr of H_2 and 0.672kmol/hr of N_2 are coke oven gas (COG) composition and moisture content. For instance, 20% - 30% of CH_4, 5% - 10% of CO, 45% - 64% of H_2, 7% of N_2, 2% - 5% of CO_2 and 0.1% - 4% of O_2 are the gas composition of coke oven reported in the literature [32] [33] [4]. The gas released from the BF includes 4% H_2, 25% CO and 20% CO_2. Other feedstock for the proposed model includes H_2O for steam and distilled H_2O production and CaO for CO_2 by-product capture through the absorption method.

Simulation set-up: Conventional and solid type for material selection in the property set-up. Mixed and conventional inert (CI) substreams. Normal distribution function type and logarithmic mesh for particle size distribution (PSD). Peng-Robinson equation of state solver for property method of thermal units. Non-random two-liquid (NRTL) method for proper electrochemical reaction in the stack which allows movement and migration of charged ions in anode and cathode sides.

Simulation method for iron and steel production: Pyrolysis of coal using H_2 as fuel and O_2 as oxidant produces syngas for the WGS unit and coke for BF. The oven (heater) was used to model the coal pyrolysis using the syngas composition stated above at 800°C operating temperature. The COG was derived from the simulated pyrolysis of coal. The evaporated syngas leaving the coal oven

mixes with syngas from the BF and BOF. Iron ore (Fe_2O_3) and limestone ($CaCO_3$) feedstock in the Fe-CaO oven-sinter were reduced and palletised to allow the exit of impurities and CO_2 which was captured. The Fe_2O_3-$CaCO_3$ thermal decomposition and sintering process of producing iron (FE) and calcium oxide (CaO) at 800°C operating temperature requires a separator. The separator removes impurities and other by-products such as Si, Mg, sulphur, phosphorous and others before reacting with the coke in the BF. Both H_2 as fuel and O_2 as oxidant were burnt in the Fe-CaO oven-sinter to eliminate the CO_2 emission footprint. The sinter by-products and coke from the coke oven react with some fraction of O_2 in the BF to produce molten iron feedstock to the BOF. In the BOF, molten steel was produced by utilising BF by-products, scrap steel and pressurised O_2 feedstock. The presence of pressurised O_2 in the BOF allowed the formation of CO and the reduction of carbon content in the molten steel. Oxy-hydrogen firing were utilised to reach the operating temperature of the BF which is 1300°C and the reaction temperature (1600°C) of the BOF. The application of heat exchangers for thermal energy recovery transformed H_2O into steam for WGS and distilled H_2O for the PEMEC stack. In the WGS (high-temperature shift (HTS) and a low-temperature shift (LTS)) unit, CO from the coke oven, BF and BOF react with steam to produce CO_2 and increase the rate of H_2 concentration. Heat exchangers before and after the first temperature shift reactor allowed proper control of CO and H_2 temperature. The by-product H_2 from the WGS unit was separated from other synthetic gas in the pressure swing adsorption (PSA) column at high purity. To eliminate the need for ASU for O_2 production and increase the H_2 production rate, renewable-powered PEMEC was incorporated. Unlike current electrolysis of H_2O systems that rely on purchased distilled H_2O, PEMEC of this proposed model utilised deionised H_2O feedstock from the cooler block to produce H_2 and O_2 with the applied voltage <1V at an operating temperature of 80°C. Produced H_2 and O_2 were fuel, oxidant and feedstock for the coke oven, Fe-CaO oven-sinter, BF and BOF.

Numerical simulation of H_2 combustion to produce thermal energy for feedstock decomposition. Coke, CaO, molten iron and steel production considered a rigorous reactor (RGibbs) with H_2 as furnace fuel to produce the required heat. A further investigation of lean burn H_2 was performed in Ansys Workbench using three-dimensional (3-D) equilibrium Navier-Stokes equations and a feasible (realisable) standard wall functions k-ε model. The reaction of BF by-products in the BOF considered an Euler-Euler multiphase solid and gas to produce molten steel and at the same time releases syngas for WGS units. The conservation of energy, momentum, species transport and thermal nitric oxide (NO) equations for the H_2 combustion, steam generation from molten steel cooling unit and Euler-Euler multiphase (solid and gas phases) are given in Eqs 13 – 18.

$$\frac{\partial}{\partial t}+\frac{\partial}{\partial x_i}(\rho u_i)=0\ (Continuity). \quad 13$$

$$\frac{\partial}{\partial t}(\rho u_i)+\frac{\partial}{\partial x_i}\left(\rho u_i u_j-\tau_{ij}\right)=\frac{\partial_p}{\partial x_i}\ (Momentum). \quad 14$$

$$\frac{\partial}{\partial t}\left(\rho u_j\right)+\frac{\partial}{\partial x_i}\left(\rho h u_j\right)=\frac{\partial(\lambda_f \partial T_f}{\partial x_i}-\sum_j \frac{\partial\left(h_j J_j\right)}{\partial x_i}+\ \sum_j h_j R_j\ (Energy) \quad 15$$

$$\frac{\partial}{\partial t}(\rho_s c_s T_s)+\frac{\partial}{\partial x_i}\left[\lambda_s \frac{\partial T_s}{\partial x_i}\right]=0\ (Energy) \quad 16$$

$$\frac{\partial(\rho Y_i)}{\partial t}+\frac{\partial(\rho u_i Y_i)}{\partial x_i}=\frac{\partial J_i}{\partial x_i}+R_i\ (Species) \quad 17$$

$$W_t=\left[4.5\frac{[10^{13.5}*m^{1.5}]}{mol^{0.5}.s}\right]\exp\left[\frac{-69466K}{T}\right]c_{O_2}^{0.5}c_{N_2}\left(\frac{T}{1K}\right)^{-0.5} \qquad (Thermal\ NO) \quad 18$$

Where: ρ = fuel (H_2) density; u = velocity; τ_{ij} = stress tensor; h = enthalpy; J_i = species i heat capacity; T = temperature; R_j = net rate for species j chemical reaction; Y_i = mass fraction of species i; λ = thermal conductivity; f = working fluid; s = solid wall; c_{N_2} = nitrogen molar concentration; p = pressure.

Solar and wind renewable energy systems. The solar array model includes a photovoltaic (PV) array and inverter for conversion of direct current (DC) to alternating current (AC). While an electron-hole relative to radiation incident was created by solar cells' absorption of photon energy greater than the energy of the band gap of the semiconductor to generate DC [34]. Eqs 19 – 23 written below describe the solar cell model.

$$I=I_{PV}-I_D \quad 19$$

$$I_D=I_0\left[exp\frac{V}{AV_T}-1\right] \quad 20$$

$$I=I_{PV}-I_0\left[exp\frac{V}{AV_T}-1\right] \quad 21$$

$$I = \left[exp\left(\frac{V + I * R_s}{I_{PV} -, 0^{*V}T}\right) - 1\right] \quad 22$$

$$P = V\left\{I_{sc} - I_0\left[exp\left(\frac{V}{AV_T}\right) - 1\right]\right\} \quad 23$$

Where

I, I_{PV}, I_D, I_0 & I_{sc} are PV output current; generated current by incident of light; bypass diode current as dependence to junction voltage; diode reverse bias saturation current; short circuit current.

V, AV_T, R_s are voltage; ampere voltage climate temperature; series resistance.

The wind turbine has two or three or more blades to harness kinetic energy from the wind which is converted to mechanical energy and finally to electrical energy in DC form. Eqs 24 and 25 represent the captured power by the wind turbine and the amount of the aerodynamic torque.

$$P_w = 0.5C_p\rho * A * V_w^3 \quad 24$$

$$T_w = P_w W_w \quad 25$$

Where

P_w, C_p, ρ, A & V_w are power derived from a wind turbine; coefficient of performance; air density; covered area by the blade rotor.

T_w & W_w are aerodynamic torque; turbine rotor speed [34] [35].

The early stage of solar and wind turbine systems development was carried out in SAM-NREL (system advisory model-national renewable energy laboratory). The modification and inclusion of the algorithm of both solar and wind energy models to generate 20MW power for electrically powered units including the PEMEC stack was completed in Matlab. The Matlab model results for both systems were saved as mat files for the Simulink model. The electrical energy needed for the proposed system was connected in the Simulink because Simulink allows interface with AspenOne. The electrical energy from either solar cells or wind turbine systems was connected to the PEMEC stack and other units that operate with electrical energy. Table 1 lists the input parameters considered during the process modelling and simulation of both solar arrays and wind turbine (WT) systems. Table 2 illustrates Aspen Plus blocks and material flows with descriptions.

Table 1. Design parameters for wind Turbine (WT) and solar cell (SC).

Wind turbine parameters		Solar cell parameters	
Parameters	Value	Parameters	Value
Rated power	20MW	Rated power	20MW
Maximum cp	0.45	Array type	Roof mount
Cut-in wind speed	4m/s	Tilt	0°
Cut-off wind speed	25m/s	Azimuth	180°
Total system loss	18%	Total system loss	14%

Table 2: List of Aspen Plus unit operation model blocks and material streams description.

Aspen Plus Block Name	Aspen Plus Block ID	Description
Mixer	MIX	Mixes syngas from oven, BF and BOD; H_2 from PSA and PEMEC.
Splitter	SPL	Split a stream into two or more. Split H_2O stream into 2 for WGS and distillation.
Hierarchy	WGS/PEMEC/SEP	Container for directories. Act as a subsystem having a set of blocks that are grouped into a single hierarchy block. House RGibbs for electrochemical separation of deionised H_2O into H_2 & O_2 with an ID name "PEMEC". House WGS for HTS and LTS.
Heat exchanger	HX	Transfers heat from one medium to another. For steam generation and H_2O distillation.
Cooler	Q_L	Thermal and phase state changer. For product cooling.

Heater	COKE-OVE/FECAO-O	For feed preheating. FECAO-O is the same as Fe-CaO oven-sinter to produce Fe, CaO and gases before the mixing of solid by-products in the sinter.
Separator	PSA/SEP	Split/separate products based on specified flows/fractions. Separate H_2 gas from others. Separate BF feed from syngas.
Rigorous reactor (RGibbs)	OVEN/DECOMP/COKE-OVE/BF/BOF/WGS/ CO_2- CAP/H_2	Set the composition of product/syngas by chemical equilibrium restriction. Gibbs free energy reactor. To produce molten iron and steel. For H_2 and CO_2 production.
Pump	PUMP	Increase feed pressure to the desired level. More effective in liquid phase.
Flow valves/controller	SPLIT-2	To estimate the required mass flowrate of H_2 fuel and O_2 oxidant for individual units (coke oven, Fe-CaO oven-sinter, BF and BOF).
Fuel-switch	F-SWITCH	Enable the use of one furnace block at a different mass flowrate of H_2 and O_2.

Aspen Plus stream ID	Description
FE	Feed.
SEP-FE	Gas separator feed.
SINT-FE	Iron (FE) and CaO feed to the BF.
COKE-FE	Coke feed to the BF.
BF-EX	Gas and slag to the separator.
BOF-FE	Molten iron feed to the BOF.
DE-COAL	Decomposed coke.
STEEL/any stream with STEEL	Steel by-product.
H_2O/any stream that starts with /end with H_2O	Water (H_2O) stream.
G-OUT/any stream that starts with G-	Syngas from coke oven, BF and BOF.
HOT-GAS/ any stream that has GAS	Synthetic gas.
BY-H_2/H_2-BY	Hydrogen (H_2) by-product.
BY-CO_2/CO_2-BY	Carbon dioxide (CO_2) by-product.
OVEN-FUE	Mass flowrate of both H_2 fuel and O_2 oxidant for coke oven.
SINT-FUE	Mass flowrate of both H_2 fuel and O_2 oxidant for Fe-CaO oven-sinter.
BF-FUE	Mass flowrate of both H_2 fuel and O_2 oxidant for BF.
BOF-FUE	Mass flowrate of both H_2 fuel and O_2 oxidant for BOF.
H-SINT/H-OVEN/H-BF/H-BOF	Thermal energy from H_2 furnace to meet the operating temperatures and heat duties.

2.1 Process simulation of iron and steel production coupled with PEMEC.

Aspen Plus software was utilised for the development of the proposed system (solar and wind aided H_2-fuelled BF-BOF coupled with PEMEC and CO_2 capture). Peng-Robinson and NTRL were both used as method solvers for proper prediction of physical and chemical reactions of the model because of the presence of charged species during the hydrogen and oxygen evolution reactions. Another free-water property methods utilised during the process simulation of the proposed model are steam-table and ideal at a water solubility of 3 for proper adjustment and accommodation of pressure drops. Below are the assumptions considered during the process development and simulation of the proposed system:

- All processes are in steady state condition.
- Intake feed temperature and pressure are ambient and atmospheric conditions.
- The pressure drop at each stage is minimal.

- H_2 flammability range ranges from 4% - 75% in air [36] [37] [38].
- 13:1 O_2 - H_2 mass ratio which is equivalent to 62:1 air to H_2 ratio.
- Electrolysis of H_2O to generate over 60% of H_2 fuel for the proposed system.
- Utility considered EU-2007/589/EC data source with natural gas as the fuel source for estimation of CO_2 emission.
- 0.85 for CO_2 energy source efficient factor and 42MJ/kg heating value for the ovens and furnaces.
- 0.58 for CO_2 energy source efficient factor and 42MJ/kg heating value for electricity at 0.117$/MJ purchased price.
- CO_2 capture by CaO absorption.

The process of making steel in the proposed system displayed in Fig. 2 starts by heating the coal in the coke oven without O_2 to produce coke for the BF. The gas and tar separators (gas-sep and sep-3) separate coke from other by-products, and coke oven gas (COG) from other end-products and tar from other impurities. Iron ore (Fe_2O_3) and limestone ($CaCO_3$) were both heated in the Fe-CaO oven-sinter to produce iron (FE) and calcium oxide (CaO) for the BF. CO_2 and other impurities were removed from the process by CO_2 separator (CO_2-sep). The endothermic reaction of Fe-CaO oven-sinter and coke oven feeds in the presence of O_2 produced molten iron, off-gas and other impurities in the BF. Separator 4 (sep-4) separates syngas from other by-products and mixes with COG in the mixer (mix-1). Impurities such as slags were excluded from the molten iron feed to the BOF. The molten steel was produced in the BOF with the presence of high-pressured O_2 and the addition of scrap metal coolant. Separator 6 (sep-6) separate BOF-syngas from other by-products and molten steel from slags and other impurities. Followed by the application of casting, rolling and sanding or reeling for the final steel production. Furnaces, syngas and molten steel cooling by H_2O in heat exchangers generated steam for WGS and distilled H_2O for the PEMEC feedstock. Cooled syngas mainly of CO at operating temperatures of 350°C for HTS and 250°C for LTS react with steam (H_2O_{gas}) to produce CO_2 and increase H_2 concentration rate. The produced H_2 and CH_4 are separated from CO_2 and other by-products like nitrogen (N_2). To maximise the H_2 production rate, renewable electricity powered PEMEC using cooled denoised H_2O feedstock from distillation boiler, produced more H_2 in the cathode side and O_2 in the anode side. O_2 from the PEMEC stack was used as the feedstock for BF and BOF and oxidant during heat production. While H_2 by-product as fuel for ovens and furnaces. CO_2 by-product from the PSA and the CO_2 separator (CO_2-sep) units was captured by exothermic reaction with CaO to produce $CaCO_3$. Recovered thermal energy from $CaCO_3$ formation can be utilised for more bio-syngas production which may be needed to recover CaO during underground storage of CO_2 by-product. Thermal utilities for coke oven, Fe-CaO oven-sinter, BF and BOF using natural gas were created to calculate the amount of CO_2 emission that can be prevented by using produced H_2 as fuel and O_2 as the oxidant. While electricity utility for the PEMEC stack and other electrically operated units was also created to estimate the amount of CO_2 emission that can be avoided by using either solar or wind energy depending on the location of the steel making plant.

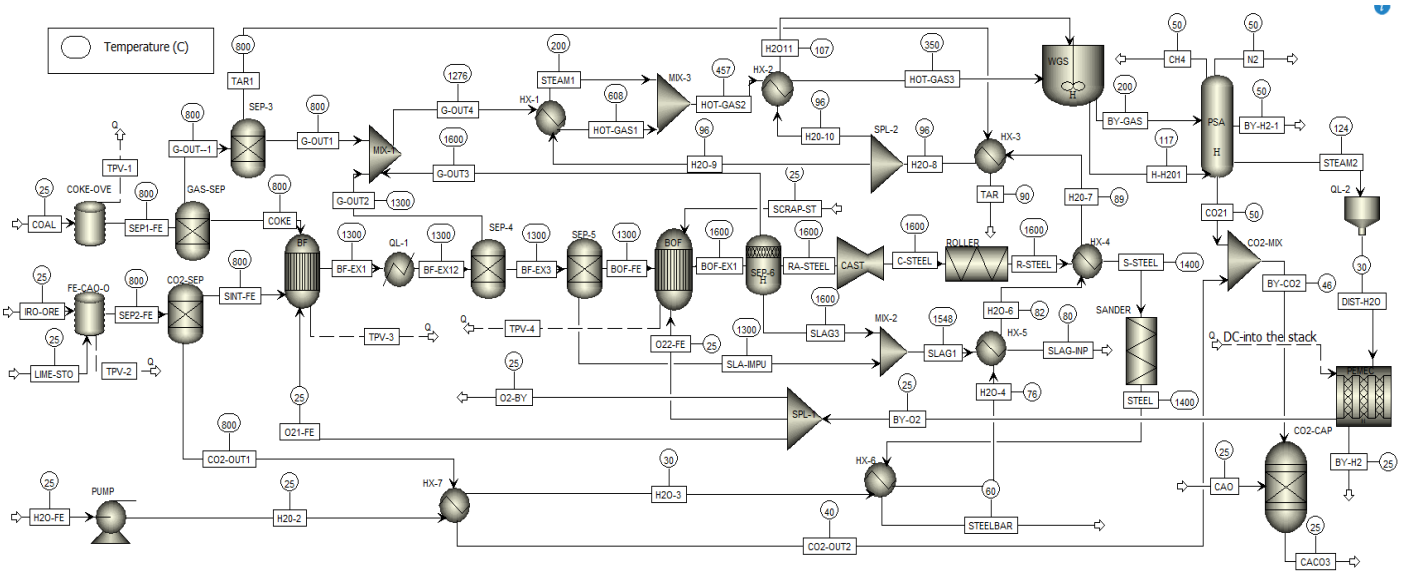

Fig 2: ASPEN Plus flow diagram for H_2-fuelled BF-BOF coupled with PEMEC and CO_2 capture.

2.2 Numerical study of hydrogen combustion, thermophotovoltaic, solar and wind energy systems for thermal and electricity production.

The diagram shown in Fig. 3a illustrates the process of utilising by-product H_2 as fuel and O_2 as the oxidant to meet the thermal energy requirement for ovens and furnaces. H_2-oven was operated at 200°C to estimate the mass flowrate of both H_2 and O_2 required to produce 2064.4MJ/hr heat duty due to losses in the production of steam and distilled H_2O. Similar procedures were applied for the estimation of mass flowrate of H_2 fuel and O_2 oxidant for ovens and furnaces at 800, 1300 and 1600°C operating temperatures in Aspen Plus. The numerical study of H_2 lean combustion in Ansys Workbench considered BOF as similar procedure can be applied to other units. The meshing of the H_2-fuelled BOF adopted face, sizing and refinement meshing types and an element number of 678652 cells was utilised. At this cell number (678652), $>10^{-6}$ energy equation and other convergence criterion equations were achieved and increased element number gave almost the same result. Thus, an element number of 678652 cells was adopted for the numerical study of H_2-fuelled BOF for molten steel production. The boundary condition for H_2-furnace to generate heat for molten steel production considered air and fuel inlets, pressure outlets for exhaust gas and evaporated syngas from the BOF and reflective non-slip walls under ambient temperature and atmospheric pressure conditions. A density of 626 kg/m^3 and a velocity magnitude inlet were applied for Euler-Euler multiphase solid and gas studies on molten steel production in the BOF. However, solid and syngas by-products of BOF were neglected as it has been studied in Fig. 2. Nonetheless, the inlet parameter considered a velocity magnitude of 0.31m/s for the molten steel. The method solver considered the second-order implicit transient formulation at the solid volume fraction phase of 0.5 for the exit molten steel to the cast or roller unit. An illustration of H_2 lean combustion to produce heat for BOF and molten steel in the BOF is given in Fig. 3b.

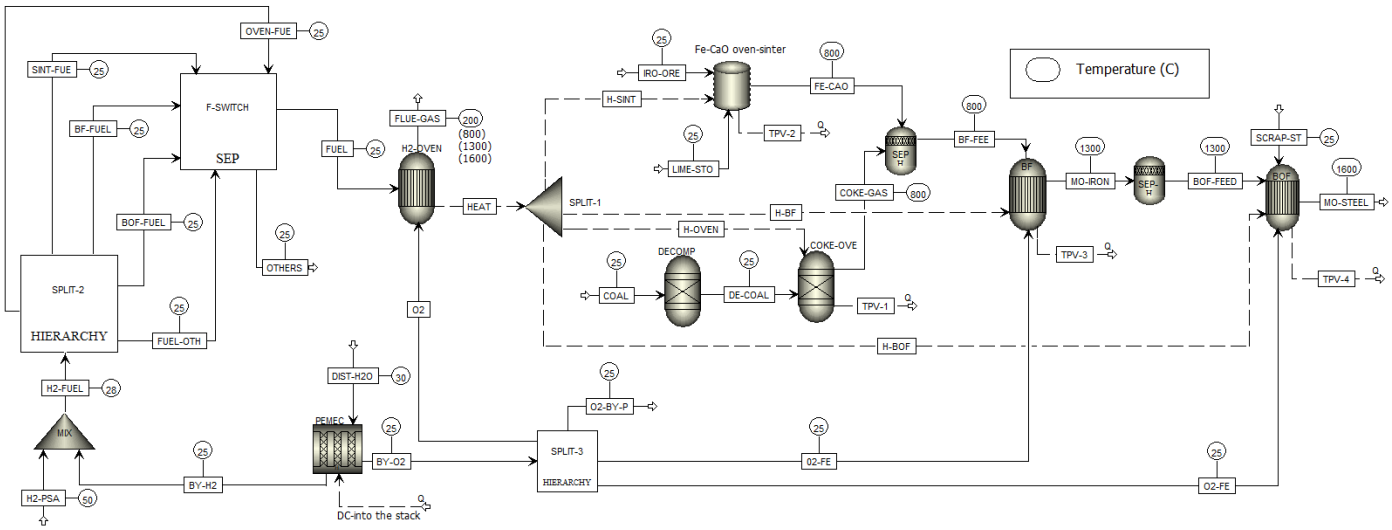

Fig 3a: ASPEN Plus flow diagram for estimation of mass flowrate of H_2 fuel and O_2 oxidant for ovens and furnaces.

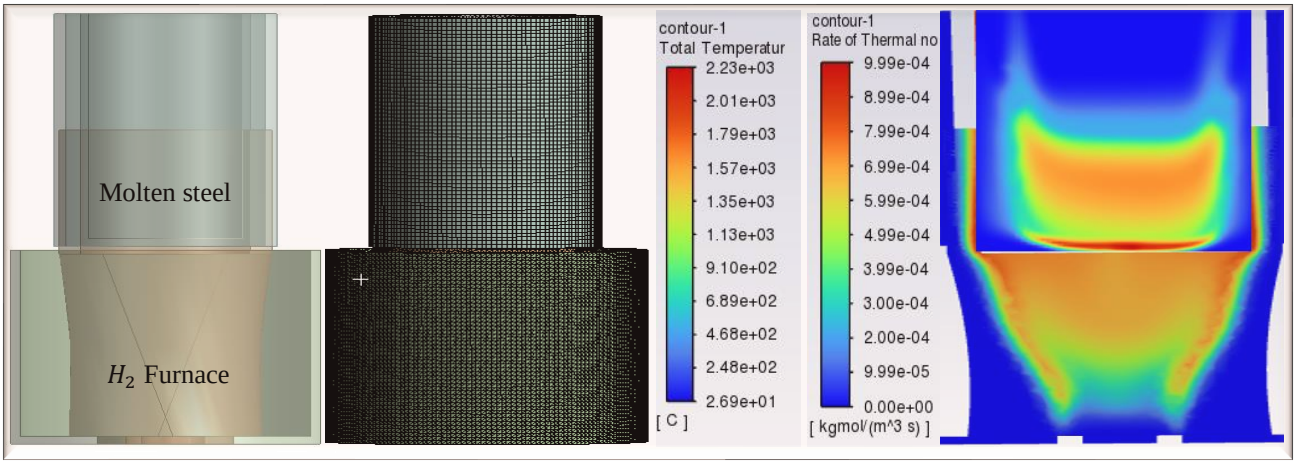

Fig. 3b: H_2 lean combustion in the BOF burner.

To demonstrate the steam generation from cooling the molten steel from the roller or sander unit, a hollow heat exchanger was modelled and simulated under laminar flow conditions. Inlet, outlet and wall are the only boundary conditions. Fig. 4 depicts steam production during the cooling of hot-rolled steel by-product. As displayed below, a heat exchanger with a few millimetres hollow distance from the rolled molten steel was utilised to transform H_2O into steam for the low-temperature PEM electrolysis of H_2O. This has been demonstrated in Fig. 2 above using an Aspen Plus process simulation software. However, Ansys Fluent was used to properly investigate the fluid absorption characteristics because of the complex nature of the steel-making process in BF-BOF as regards to waste energy recovery units.

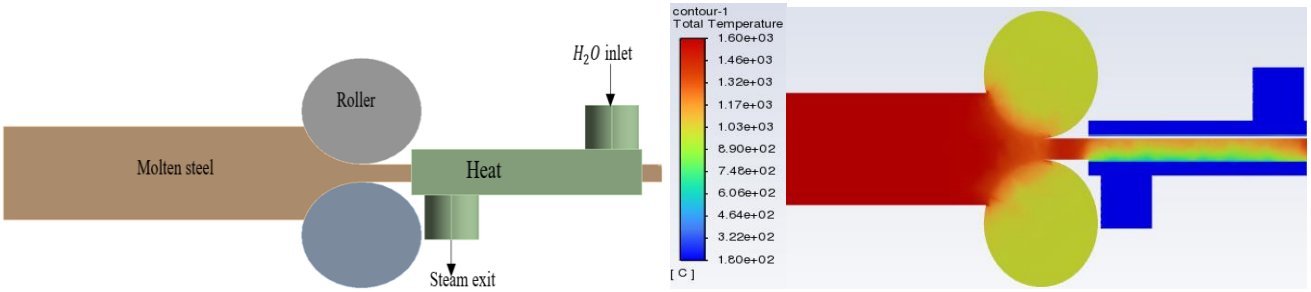

Fig 4: Steam production during the cooling of hot-rolled steel.

To maximise the electrical energy recovery, thermophotovoltaics (TPVs) units were integrated into the hybrid system. Copper alloy, chromium and stainless steel are the list of materials considered for waste heat to electricity conversion via TPV system. Copper alloy as the emitter and heat sink material for ovens. p-type and n-type materials for electrons' donor and acceptor. $1.46 W m^{-1} C^{-1}$ thermal conductivity and -0.000187 isotropic seebeck coefficient for n-type and $1.46 W m^{-1} C^{-1}$ thermal conductivity and 0.000187 isotropic seebeck coefficient for p-type are the properties of both materials. Chromium and stainless steel materials for BF and BOF emitter, and copper alloy for heat sinks. These materials were fitted on both ovens and furnaces' walls to generate electricity. In TPV cells, heat from the ovens and furnaces is transferred to the copper alloy (emitter) and electricity is generated by the thermal radiation of emitters. As copper alloy melting temperature is within 1050°C, both stainless steel and chromium for higher temperature furnaces were used as mechanical supports. Fig. 5 displays a TPV converter fitted on a coke oven, Fe-CaO oven-sinter, BF and BOF walls. The efficiency of TPV can be calculated using Eq 26. TPV efficiency is the power output ratio of TPV cells (P_{EL}) to the net thermal output of the emitter ($P_{out} - P_{in}$).

$$n = n_{th} * n_{TPV} = \frac{P_{out} - P_{in}}{Q_{in}} * \frac{P_{EL}}{P_{out} - P_{in}} \quad (26)$$

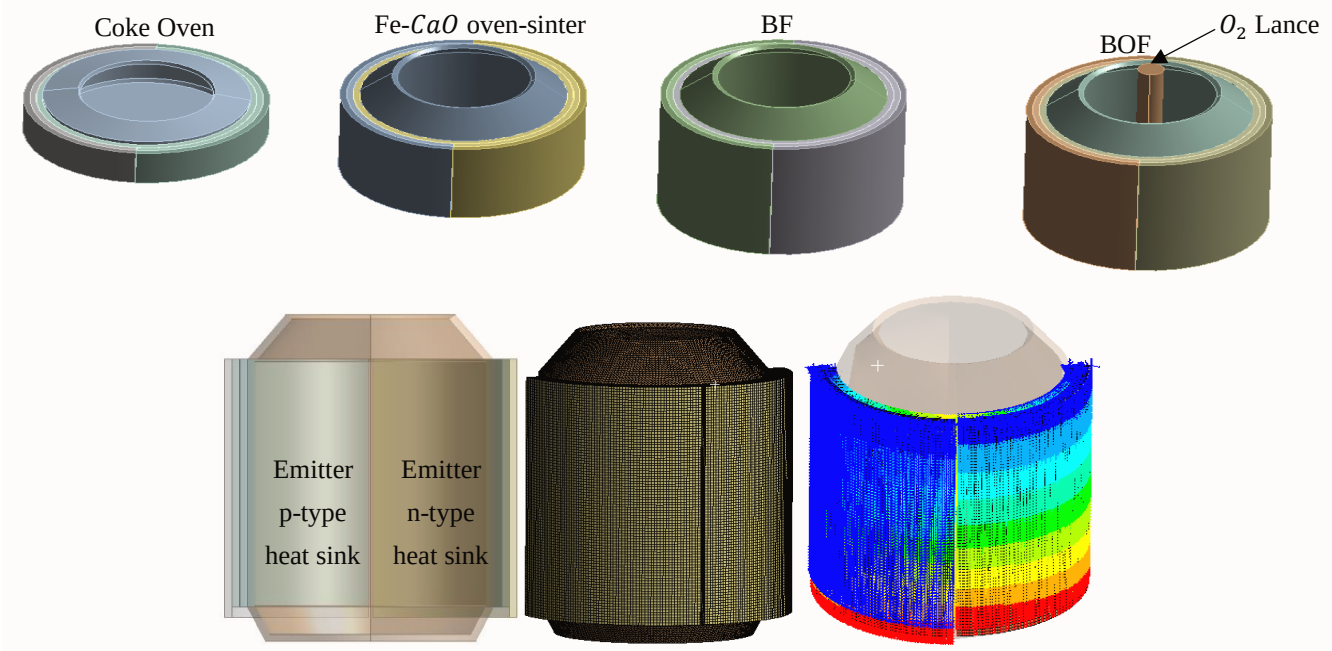

Fig 5: Thermophotovoltaic (TPV) unit of coke oven, Fe-CaO oven-sinter, BF and BOF.

Renewable solar cells and wind turbine (WT) systems were developed in SAM-Matlab to increase the electricity output of thermoelectric units. This is necessary because Aspe Plus is limited to the development of renewable solar or wind energy. The simulated Aspen Plus model in Fig. 2 was transformed into flow-driven for the Simulink interface as shown in Fig. 6 to utilise the generated electricity from either solar or wind energy systems. In the displayed Simulink model, a switch was introduced to demonstrate the flexibility of using either solar or wind renewable energy as the electricity source of the proposed system. While electricity generated from any of these sources was connected to the PEMEC stack and other electrically powered units to have the integrated system working as a single unit. The distribution of electricity from the renewable source to other electrical units can be carried out in practice for low-carbon BF-BOF steel manufacturing plants.

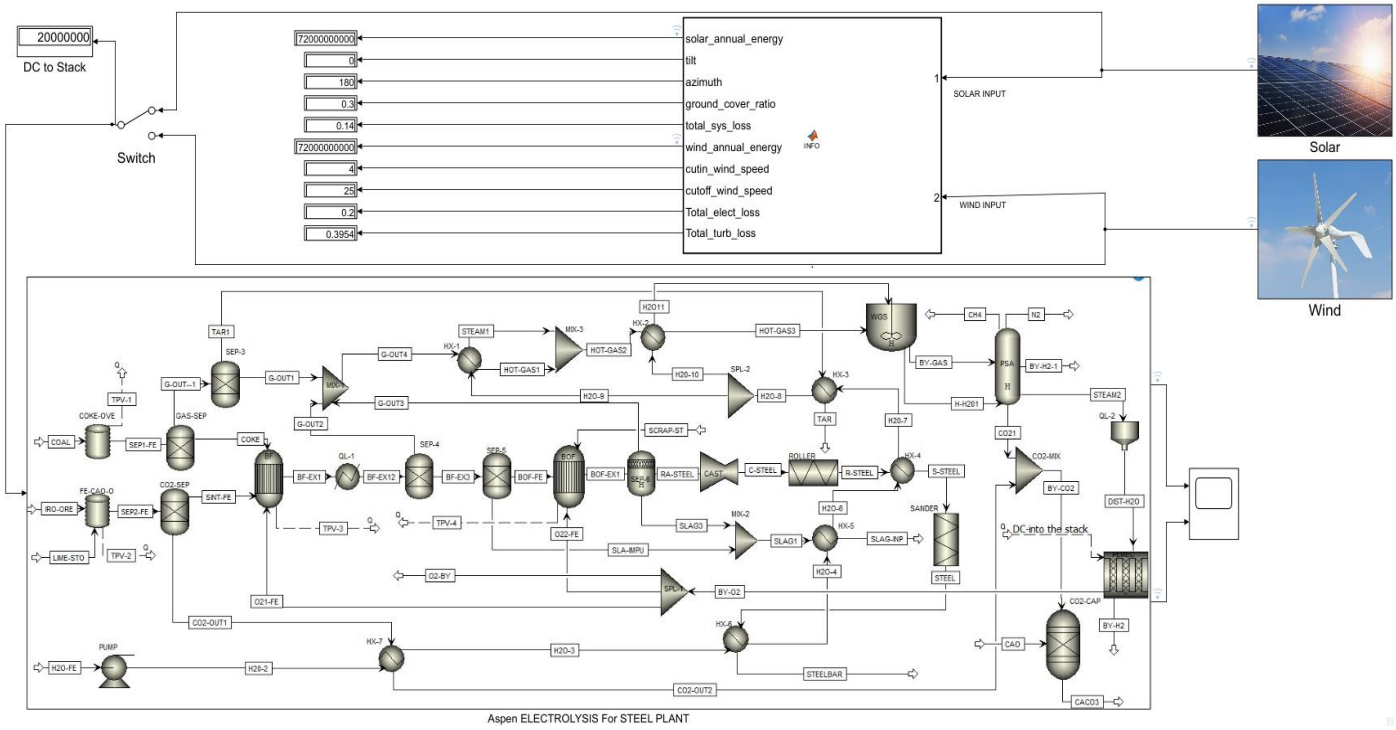

Fig 6: Solar and wind aided H_2-fuelled BF-BOF coupled with PEMEC and CO_2 capture.

3. Results and Discussions

The result of the proposed low-carbon high-quality steel plant shows that for oxy-hydrogen combustion at a ratio of 13:1, 2.4kg of natural gas is required to produce the same heat for the ovens and furnaces. It was observed that for every 626kg of produced steel, 1110.4kg of CO_2 emission can be prevented by replacing natural gas with H_2 fuel. A total of 7865.8kg of CO_2 emission can also be eliminated from the process by using solar or wind energy sources to generate 20MW power. Having stored 1290.4kg/hr of H_2 and 38.5kg/hr of CH_4, the need to burn natural gas or biomass during low wind speed or the absence of sunshine can be avoided. 2533.95kg/hr of O_2 and 1290.4kg/hr of H_2 were syngas by-products from the developed system with H_2 and O_2 as fuel and oxidant for coke oven, Fe-CaO oven-sinter, BF and BOF. The capture of CO_2 by-product (1002kg/hr) released 4077.2MJ/hr energy which can be recovered for more production of H_2 fuel needed to release CO_2 from CaO during underground storage. The introduction of TPV units for waste heat to electrical improved the energy recovery efficiency. Energy efficiency was up by >10% with the introduction of thermoelectric units and an efficiency of 82% for the PEMEC unit was achieved. While CO_2 emission footprint was removed from the process by adopting oxy-hydrogen combustion and capture of CO_2 by-product by absorption process. The utilisation of H_2 as fuel and O_2 as the oxidant for the simulated model has proven that the need for expanding current high-grade iron and steel production plants to accommodate large-scale CO_2 capture units can be avoided. By using by-product H_2 as fuel and O_2 as oxidant and solar or wind energy source, the transportation cost of natural gas to iron and steel manufacturing plants and electricity usage burden to the grid can also be prevented. Table 3 reports the thermal and electrical energy input and output, amount of CO_2 emission, biofuel and oxidant for the proposed steel plant.

Table 3: Input and output energies for individual units, amount of CO_2 emission, biofuel and oxidant for the proposed steel plant.

Units	Thermal energy input (MJ/hr)	Electrical energy input (kW)	TPV energy output (kW)	Tem (°C)	Natural gas (NG) (kg/hr)	CO_2 emission (kg/hr) with NG	Required H_2 fuel (kg/hr)	Required O_2 oxidant (kg/hr)
Coke oven	665.5		4.8	800	15.9	43.9	6.6	85.2
Fe-CaO oven-sinter	747.5		11	800	17.8	49.3	7.4	95.7
Blast furnace (BF)	5838.6		19.9	1300	139	385.4	66.8	868.2
Basic oxygen furnace (BOF)	7510.4		25.4	1600	178.8	495.7	96.4	1252.6
Others and Heat exchanges (HE)	2064.4			150 - 350	49.2	136.3	17.9	232.2
PEMEC stack		19398.8		80		6754.8		
Pressure changer		1.2				0.4		
Syngas separator/PSA		Not applicable				Not applicable		
Total	16826.4	19.4MW	61.1kW		400.7	7865.8	195.1	2533.9

3.1 Model Validation

The syngas production from the coke oven, BF and BOF of this model is validated against the data reported in the literature [39]. For instance, BF, BOF and Linz-Donawitz (LD) gases mainly of H_2, CO and CH_4 are produced during the production of steel and represent about 30% of fuel consumption [40] [41]. Unlike the existing steel-making plants, the WGS and H_2O electrolysis units were introduced to increase the H_2 production rate required to substitute natural gas or other fossil fuels for oxy-combustion. Table 4 reports model validation of the proposed system against the literature data on gas composition. Considering the syngas composition of this study with literature data, the simulated model achieved a similar result with marginal deviation. It can be seen from the validated data that the proposed work recorded lower N_2 by-product because of O_2 utilisation in the decomposing units. Comparing the performance of the PEMEC unit of the proposed system against the literature data presented by *Sapountzi, et al.* [42], it can be said that both studies reached almost the same value for efficiency. For instance, PEMEC efficiency between 65% and 82% was reported by *Sapountzi et al.* [42]. Validating the TPV unit against Zhao, et al. [30] studied work, a minimal difference was attained.

Table 4: Model validation based on gas composition.

Type	Source	Gas	Composition (%)	
			[32] [43] [44]	Present work
Coke oven gas	Coke oven	H_2 CH_4 CO CO_2 H_2O N_2/O_2 or Others	45 – 64 20 – 30 5 – 10 2 – 5 0.1 - 4	50.5 21.1 6.7 2.1 15.8 3.8
BF gas	BF	H_2 CO CO_2 N_2 or Others	1 - 4 20 - 28 17 - 25 41 - 55	19.7 80.2 0.02 0.18
	BOF	H_2 CO CO_2 Others		21.3 66.3 7.9 4.5
Linz-Donawitz (LD) gas	Converter	H_2 CO CO_2 Others	1.5 60 15 – 20 10 - 22	

3.2 NOx analysis and effect of thermophotovoltaic (TPV) heat source material on power output.

At a maximum temperature of 2000°C, $0.00061 kg/mol/m^3 s$ thermal NO (nitric oxide) and <5ppm NOx emission were recorded. The lower NOx emission of this study was attributed to oxy-hydrogen firing as this approach is considered the best way of minimising NOx formation in high-temperature applications. NOx emissions of this study can be minimised further by adding cooling units or a coolant such as steam or N_2 into the H_2 burner. NOx formation probably occurs at a higher reaction temperature as *Hoekman & Robbins* affirmed that thermal NOx formation occurs at a reaction temperature >1500°C [45]. NOx formation rate in ppm can be calculated using Eq 27 or 28.

$$\frac{(mole_{fraction}\ of\ pollutant_{NO}\ +\ mole_{fraction}\ of\ pollutant_{N_2O})10^6}{mole_{fraction}\ of\ H_2O} \quad 27$$

$$\frac{(mole_{fraction}\ of\ pollutant_{NO}\ +\ mole_{fraction}\ of\ pollutant_{N_2O})10^6}{mole_{fraction}\ of\ H_2O + mole_{fraction}\ of\ O_2\ (species)} \quad 28$$

Waste heat to electricity of this study utilised chromium for BOF, stainless steel for BF and copper alloy materials for the ovens. It was observed that at an emitting temperature of 750°C using a copper alloy as the emitter, chromium, stainless steel or tungsten emitters require emitting temperatures ranging from 1300°C to 1480°C to achieve the same power efficiency. Therefore, the use of a copper alloy as the emitting material for the TPV units mounted on BF or BOF walls with a few millimetres' gaps between both walls can be considered. The effect of TPV heat source material on the same power output of the proposed system is illustrated in Fig. 7.

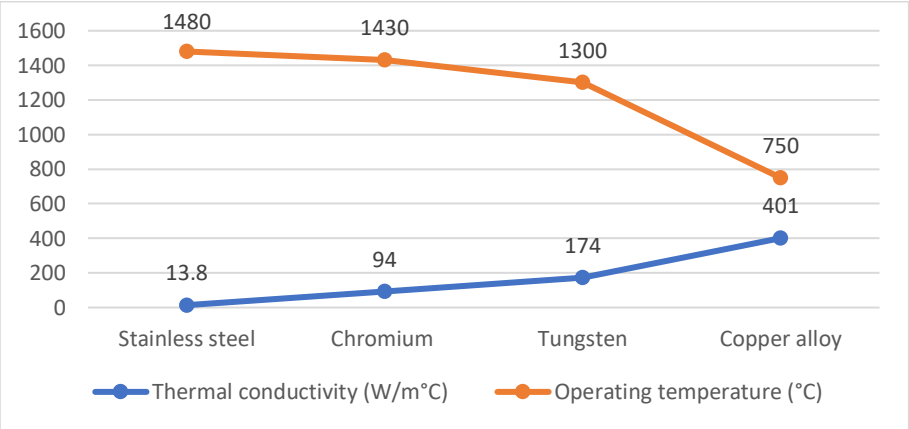

Fig 7: The effect of TPV heat source material on the same power output.

3.3 Economic analysis and environmental assessment of hydrogen as fuel in BF-BOF steel plant

Oxy-hydrogen combustion can substitute oxy-NG (natural gas) or air-NG firing at a ratio of 2.1:1 without the need for additional hydrocarbon fuels to meet the reaction temperatures and heat duties of the thermal units. This ratio of H_2 to NG increases as the reaction temperature reduces and increases with the increase in the operational temperature. H_2 blend with NG at a volume ratio of 3:1 in DRI and burning additional fuel to meet the operating temperature of the BF unit can only reduce CO_2 emission by 2.5% in the integrated DRI-BF [46]. Unlike the combustion of H_2 and NG in the DRI, oxy-hydrogen combustion at a ratio of 2.1:1 eliminated CO_2 footprint from the combustion process. In addition, H_2 injection into ovens and furnaces as a reducing agent can reduce CO_2 emission by just 21.4% [47]. With the application of thermal energy recovery through heat exchanger and TPV units, between 1.8GJ/t hrs and 3GJ/t hrs can be recovered from this proposed system. Apart from the NOx formation issue in H_2-based steel production plants, which can be mitigated by the introduction of cooling systems or replacing existing NG and biomass furnaces with a H_2 burner, the cost of H_2 fuel compared to other fossil fuels remains another challenge. For instance, NG costs between \$2.6/MMBtu - \$2.9MMBtu, while H_2 cost depends on the production method. Blue H_2 sales price is between \$2.2/kg and \$2.9/kg and green H_2 from electrolysis costs from \$5.10/kg - 10.3/kg [48] [49]. This shows that blue H_2 from hydrocarbon reforming with carbon capture and storage (CCS) unit and H_2 from renewable sources such as pyrolysis with \$1.18/kg - \$1.89/kg H_2 selling price remain the viable replacement option for NG in steel-making plants. The high cost of green H_2 is attributed to the use of distilled H_2O, electricity from the grid and metal electrocatalyst or cell stack configuration. For example, at $\$3.89/kg/_{H_2}$, H_2O desalination

(production of deionised H_2O) costs $0.084. Thus, replacing grid electricity with solar or wind sources of electricity and producing distilled H_2O feedstock at the site of operation will reduce the cost of H_2 from the electrolysis method. This proposed system has applied both mitigation points by utilising recovered thermal energy to produce deionised H_2O feedstock for the PEMEC stack and replaced grid electricity with electricity from solar or wind sources. This shows that with an appropriate site location where solar or wind renewable energy sources and other raw materials are available, this simulated model can achieve deep decarbonisation and cost competitive compared with the existing steel production plants. Besides, an energy efficiency higher than the current BF-BOF steel plant was achieved. Biomass coke for replacing coal coke for BF has been suggested for carbon reduction in high-grade steel production as mentioned in the above literature review. For example, pyrolysis of biomass for charcoal production can be achieved at lower operating temperatures compared to coal pyrolysis [50] [6]. However, issues related to land-use change (LUC), life-cycle assessment (LCA), low syngas production at lower pyrolysis temperatures (300°C – 400°C) and higher cost limits such transition. Comparing this model that uses blue and green H_2 for ovens and furnaces with an existing steel production plant that relies on biomass fuel, zero CO_2 emission is possible. As mentioned by *Mandova et al.*, reduction in CO_2 emission in biomass-based steel production plants can only achieve between 25% and 58% which does not lead to full decarbonisation [51]. Application of this proposed system in high-grade steel plants will minimise the rapid growth of EAF as more scrap recycling can be accommodated because of the higher H_2 fuel flammability limit (4% lower and 75% upper) [52]. The implementation of this innovative proposed system recommends the use of solar energy in countries that experience longer sunshine and wind energy in European countries. For instance, the transition to offshore and onshore wind in European countries like the United Kingdom remains the best route towards meeting the zero carbon emission target by 2050 [53]. Fig. 8 reports capital, operation and maintenance costs (a) and utility savings (b) for the proposed system. The illustrated capital cost and utility savings were calculated as a reference to Fig. 2.

Total Capital Cost [USD]	4,213,640
Total Operating Cost [USD/Year]	1,888,280
Total Raw Materials Cost [USD/Year]	0
Total Product Sales [USD/Year]	0
Total Utilities Cost [USD/Year]	579,137
Desired Rate of Return [Percent/'Year]	20
P.O. Period [Year]	0
Equipment Cost [USD]	243,000
Total Installed Cost [USD]	1,233,900

(a)

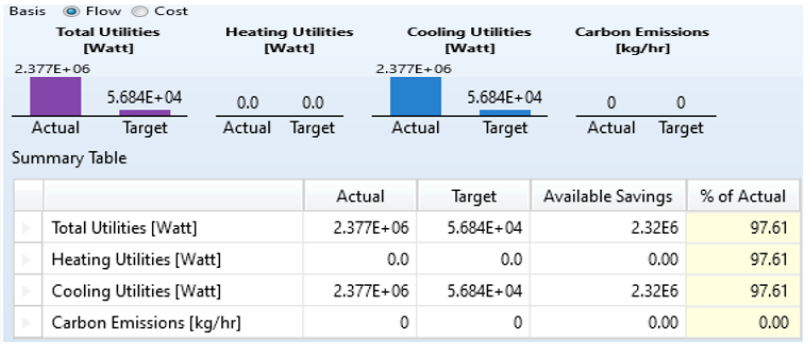

Summary Table

	Actual	Target	Available Savings	% of Actual
Total Utilities [Watt]	2.377E+06	5.684E+04	2.32E6	97.61
Heating Utilities [Watt]	0.0	0.0	0.00	97.61
Cooling Utilities [Watt]	2.377E+06	5.684E+04	2.32E6	97.61
Carbon Emissions [kg/hr]	0	0	0.00	0.00

(b)

Fig 8: Capital, operation and maintenance costs (a) and utility savings (b) for the proposed system.

3.4 Comparison of this proposed low-carbon steel production plant with similar technologies operating with CCS units and its limitations.

This study applied low-temperature electrolysis to utilise the generated electricity from the thermoelectric, solar or wind power systems for both H_2 and O_2 production. By producing ovens and furnaces low-carbon fuel (H_2) at the site of operation, the technical issues associated with large-scale carbon capture and storage (CCS) units were prevented. Despite the high cost of biohydrogen or green H_2 in contrast to blue or grey H_2, the operational cost of this proposed system (BF-BOF route of green steel production) will be reduced. For instance, CO_2 capture from plants costs between $12 - $94/tonne and deionised H_2O feed to the electrolysis costs $\$0.084 kg_{H_2}$ [54]. The only by-product CO_2 of this study came from the thermal decomposition of $CaCO_3$ to recover CaO and the conversion of CO from the coke oven and furnaces to CO_2 in both high-temperature and low-temperature shifts (WGS unit). This shows that between $12 and $50 can be saved by substituting this proposed system with the current BF-BOF route operating with a CCS unit as $7865.8 kg_{CO_2}$ was prevented. The operational cost be further minimised when operated in regions with a carbon tax policy. For example, a carbon tax between $20 – $80/tCO_2$ has been suggested to decarbonise high-carbon emitting sectors [54]. Furthermore, CO_2 transportation to storage sites can further increase operation cost of low-carbon steel operating with a CCS unit. For instance, comparative studies of CO_2 transport methods show that long-distance transport of CO_2 by ships and pipelines costs more and CO_2 transport by pipelines has several issues such as corrosion, pressure loss and new infrastructures [55] [56] [57]. The

proposed system implemented CO_2 by-product capture by the absorption process which requires minimal installation space and is easy to transport by truck or ship, which is cheaper than the pipeline mode of CO_2 transport [58].

The size of this developed model can be maximised to increase green steel production rate. The increase in steel production capacity means that more energy can be recovered from the ovens and furnaces' walls via thermoelectric applications. Furthermore, more H_2, CH_4 and O_2 can be produced as more heat will be released from the ovens and furnaces under the same operating temperature and pressure conditions. However, increasing the production of green steel requires more installation of solar cells or wind turbine renewable energy systems for the electrolysis of H_2O. Nevertheless, a minimal increase of feedstock to produce more green steel does not require an increase in solar or wind power capacity as more H_2 fuel was unused, and the generated electricity from both renewable sources was more than enough for the electrical units. In addition, the electricity obtained from thermoelectric units was unused. Thus, keeping the same density of green steel by-product may require a reduction of solar or wind installation capacity. In reference to the size of each component of the developed system, the size of the BF-BOF plant operating on higher feeds can be estimated. For instance, increasing the coke oven feed by a factor of 2 means doubling the oven volume for proper thermal decomposition of coal to release coke feed to BF. This developed system is limited to high-temperature electrolysis of H_2O because of the complexity of waste heat to high-temperature steam substrate. Other limitations include blending H_2 fuel with other fuels except for CH_4 or NG as the oxy-hydrogen firing burner was developed for the H_2 fuel with the flexibility of accommodating lightweight and high energy density fuels. One of the drawbacks of the proposed system is the higher cost of steel in contrast to the traditional route operating with fossil fuel burners without a CCS unit. Nonetheless, it can be operated in any region where solar or wind is unavailable but other renewable power systems are present. The proposed system is designed for high-grade steel production but not limited to low-grade steel by recycling more scrap steel in the BOF. Below are some of the advantages of the developed system.

a) Absence of CO_2 emission and the production of blue and green H_2 at the site of operation.
b) Natural gas or biomass substitution with the produced H_2 by-product from both WGS and PEMEC stack.
c) Renewable energy sources for electrical units and use of by-product O_2 as feedstock and oxidant (oxy-firing).
d) Low by-product CO_2 production and CO_2 capture by absorption process.
e) Cheaper operational cost compared to conventional steel-making plants operating with a CCS unit.

4. Conclusion

H_2-fuelled BF-BOF route coupled with a renewable-powered PEMEC system for high-grade steel production was developed and simulated for the reduction of carbon emission footprints. By reacting CO_2 with CaO to form $CaCO_3$ and the use of solar or wind renewable energy sources, CO_2 emission into the environment was prevented. With 20MW power output from either solar or wind renewable sources, the developed model produced excess H_2 fuel and O_2 oxidant and feedstock needed during cloud-covered periods and low wind speed. 38.5kg/hr of CH_4 recovered from pyrolysis of coal was unused which can be stored as backup fuel or can be sold to recover investment cost. Application of steam and distilled H_2O production for WGS and PEMEC feedstocks through heat recovery eliminated the need for purchasing deionised H_2O which cost about $\$0.084 kg_{H_2}$. By capturing the by-product CO_2 (1002kg/hr) from the syngas separation column via the absorption method and by preventing $7865.8 kg_{CO_2}$ through the introduction of oxy-hydrogen firing burners and the renewable power source, the operational cost was reduced as CCS units' costs between \$12 - $\$94/tonne/_{CO_2}$. The introduction of TPV units recovered 61.1kW from ovens and furnaces. By comparing the simulated model with literature data, a minor deviation was recorded. The proposed system achieved energy efficiency ≥10% and lower steel sales price in comparison with the conventional BF-BOF route operating with a CCS unit. However, the developed system is limited to high-temperature electrolysis of H_2O due to the complexity of the heat recovery in molten steel cooling unit. To accommodate the recycling of more scrap metals in the high-grade steel making route (BF-BOF), as well as removing CO_2 emission from the process, this proposed system recommends a pilot-scale development utilising renewable energy sources available at the chosen site location.

Declaration of Competing Interest

The authors declare that they have no known competing financial interests or personal relationships that could have appeared to influence the work reported in this paper.

References

[1] IEA, 2020. *Iron and Steel Technology Roadmap.* Available at: https://www.iea.org/reports/iron-and-steel-technology-roadmap.

[2] Bataille, C., P.Eng, S. S. & CEng, F. G. N. L., 2021. *Global Facility Level Net-Zero Steel Pathways: Technical Report On the First Scenarios of the Net-zero Steel Project.* Available at: http://netzerosteel.org/wpcontent/uploads/pdf/net_zero_steel_report.pdf: IDDRI.

[3] Pauliuk, S., Milford, R. L., Müller, D. B. & Allwood, J. M., 2013. The Steel Scrap Age. *Environmental Science & Technology,* 7, p. 3448 – 3454.

[4] Zhang, Q., Zhao, X., Lu, H., Ni, T., & Li, Y., 2017. Waste energy recovery and energy efficiency improvement in China's iron and steel industry. *Applied Energy,* 191, pp. 502 - 520.

[5] Tarrés, J., Maas, S., Scholzen, F. & Zürbes, A., 2014. Simulated and experimental results on heat recovery from hot steel beams in a cooling bed applying modified solar absorbers. *Journal of Cleaner Production,* 68, pp. 261 - 271.

[6] Fan, Z. & Friedmann, S. J., 2021. Low-carbon production of iron and steel: Technology options, economic assessment, and policy. *Joule,* 5(4), pp. 829 - 862.

[7] Kildahl, H., Wang, L., Tong, L. & Ding, Y., 2023. Cost effective decarbonisation of blast furnace – basic oxygen furnace steel production through thermochemical sector coupling. *Journal of Cleaner Production,* 389, p. 135963.

[8] Ren, L., Zhou, S., Peng, T. & Ou, X., 2021. A review of CO_2 emissions reduction technologies and low-carbon development in the iron and steel industry focusing on China. *Renewable and Sustainable Energy Reviews,* 143, p. 110846.

[9] Arens, M., Worrell, E. & Schleich, J., 2012. Energy intensity development of the German iron and steel industry between 1991 and 2007. *Energy,* 45(1), pp. 786 - 797.

[10] Orth, A., Anastasijevic, N. & Eichberger, H., 2007. Low CO_2 emission technologies for iron and steelmaking as well as titania slag production. *Minerals Engineering,* 20(9), pp. 854 - 861.

[11] Zhang, J., Fu, H., Liu, Y., Dang, H., Ye, L., Conejio, A. N., & Xu, R. 2022. Review on biomass metallurgy: Pretreatment technology, metallurgical mechanism and process design. *International Journal of Minerals, Metallurgy and Materials*, 29, pp. 1133 – 1149.

[12] Dang, H., Xu, R., Zhang, J., Wang, M., & Li, J. 2023. Cross-upgrading of biomass hydrothermal carbonization and pyrolysis for high quality blast furnace injection fuel production: Physicochemical characteristics and gasification kinetics analysis. *International Journal of Minerals, Metallurgy and Materials*.

[13] Suopajärvi, H. & Fabritius, T., 2013. Towards More Sustainable Ironmaking—An Analysis of Energy Wood Availability in Finland and the Economics of Charcoal Production. *Sustainability,* 5(3), pp. 1188 - 1207.

[14] Geerdes, M., Chaigneau, R., Lingiardi, O., Molenaar, R., Opbergen, R. v., Sha, Y., & Warren, P., 2020. *Modern Blast Furnace Ironmaking – An Introduction.* 4th ed. s.l.:Ios Pr Inc.

[15] Quader, M. A., Ahmed, S., S.Z., D. & Nukman, Y., 2016. Present needs, recent progress and future trends of energy-efficient Ultra-Low Carbon Dioxide (CO_2) Steelmaking (ULCOS) program. *Renewable and Sustainable Energy Reviews,* 55, pp. 537 - 549.

[16] Arens, M., Worrell, E., & Schleich, J., 2017. Pathways to a low-carbon iron and steel industry in the medium-term – the case of Germany. *Journal of Cleaner Production,* 163, pp. 84 - 98.

[17] Toktarova, A., Karlsson, I., Rootzén, J., Göransson, L., Odenberger, M., & Johnsson, F., 2020. Pathways for Low-Carbon Transition of the Steel Industry—A Swedish Case Study. *energies,* 13(15), p. 3840.

[18] Echterhof, T., 2021. Review on the Use of Alternative Carbon Sources in EAF Steelmaking. *Metals,* 11(2), p. 222.

[19] Kirschen, M., Risonarta, V. & Pfeifer, H., 2009. Energy efficiency and the influence of gas burners to the energy related carbon dioxide emissions of electric arc furnaces in steel industry. *Energy,* 34(9), pp. 1065 - 1072.

[20] IEA, 2010. *Energy Technology Perspectives: Scenarios and Strategies to 2050.* [Online] Available at: https://iea.blob.core.windows.net/assets/04776631-ea93-4fea-b56d-2db821bdad10/etp2010.pdf [Accessed 22 06 2023].

[21] Bailera, M., Lisbona, P., Peña, B. & Romeo, L. M., 2021. A review on CO_2 mitigation in the Iron and Steel industry through Power to X processes. *Journal of CO_2 Utilization,* 46, p. 101456.

[22] Ren, L., Zhou, S. & Ou, X., 2023. The carbon reduction potential of hydrogen in the low carbon transition of the iron and steel industry: The case of China. *Renewable and Sustainable Energy Reviews,* 171, p. 113026.

[23] Hasanbeigi, A., Arens, M. & Price, L., 2014. Alternative emerging ironmaking technologies for energy-efficiency and carbon dioxide emissions reduction: A technical review. *Renewable and Sustainable Energy Reviews,* 33, pp. 645 - 658.

[24] Khan, M. A., Zhao, H., Zou, W., Chen, Z., Cao, W., Fang, J., . . . Zhang, J., 2018. Recent Progresses in Electrocatalysts for Water Electrolysis. *Electrochemical Energy Reviews,* 1, pp. 483 - 530.

[25] Kumar, S. S. & Himabindu, V., 2019. Hydrogen production by PEM water electrolysis – A review. *Materials Science for Energy Technologies,* 2(3), pp. 442 - 454.

[26] Brezak, D., Kovač, A. & Firak, M., 2023. MATLAB/Simulink simulation of low-pressure PEM electrolyzer stack. *International Journal of Hydrogen Energy,* 48(16), pp. 6158 - 6173.

[27] Devlin, A., Kossen, J., Goldie-Jones, H. & Yang, A., 2023. Global green hydrogen-based steel opportunities surrounding high quality renewable energy and iron ore deposits. *nature communications,* 14, p. 2578.

[28] BSC, I., 2008. *Waste heat recovery: technology and opportunities in US industry.* s.l.: Department of Energy (US).

[29] Datas, A., 2015. Optimum semiconductor bandgaps in single junction and multijunction thermophotovoltaic converters. *Solar Energy Materials and Solar Cells,* 134, pp. 275 - 290.

[30] Zhao, B., Chen, K., Buddhiraju, S., Bhatt, G., Lipson, M., & Fan, S., 2017. High-performance near-field thermophotovoltaics for waste heat recovery. *Nano Energy,* 41, pp. 344 - 350.

[31] Mulholland, M. D., & Seidman, D. N, 2011. Nanoscale co-precipitation and mechanical properties of a high-strength low-carbon steel. *Acta Materialia*, 59(5), pp. 1881 – 1897.

[32] Uribe-Soto, W., Portha, J.-F., Commenge, J.-M. & Falk, L., 2017. A review of thermochemical processes and technologies to use steelworks off-gases. *Renewable and Sustainable Energy Reviews,* 74, pp. 809 - 823.

[33] Flues, F., Rübbelke, D. & Vögele, S., 2015. An analysis of the economic determinants of energy efficiency in the European iron and steel industry. *Journal of Cleaner Production,* 104, pp. 250 - 263.

[34] Kanagasakthivel, B. & Devaraj, D., 2015. Simulation and performance analysis of Solar PV-Wind hybrid energy system using MATLAB/SIMULINK. *IEEE,* Chennai.

[35] Bouzguenda, M., Salmi, T., Gastli, A. & Masmoudi, A., 2012. Evaluating solar photovoltaic system performance using MATLAB. *IEEE* Nabeul.

[36] Verhelst, S. & Sierens, R., 2001. Hydrogen engine-specific properties. *International Journal of Hydrogen Energy,* 26(9), pp. 987 - 990.

[37] Abdel-Aal, H., Sadik, M., Bassyouni, M. & Shalabi, M., 2005. A new approach to utilize Hydrogen as a safe fuel. *International Journal of Hydrogen Energy,* 30(13 - 14), pp. 1511 - 1514.

[38] Jo, Y. D. & Crowl, D. A., 2010. Explosion characteristics of hydrogen-air mixtures in a spherical vessel. *Process Safety Progress,* 29(3), pp. 216 - 223.

[39] Wang, R., Jiang, L., Wang, Y. & Roskilly, A., 2020. Energy saving technologies and mass-thermal network optimization for decarbonized iron and steel industry: A review. *Journal of Cleaner Production,* 274, p. 122997.

[40] Zhang, Q., Liu, W.-c., Du, T., Cai, J.-j., Xu, C.-b., & Bai, X.-b., 2010. *Utilization Secondary Energy in Integrated Iron and Steel Works for Improving Energy Utilization Efficiency.* Changcha, IEEE.

[41] Zhao, X., Bai, H. & Hao, J., 2017. A review on the optimal scheduling of byproduct gases in steel making industry. *Energy Procedia,* 142, pp. 2852 - 2857.

[42] Sapountzi, F. M., Gracia, J. M., Weststrate, C.J., Fredriksson, H. O., & Niemantsverdriet, J., 2017. Electrocatalysts for the generation of hydrogen, oxygen and synthesis gas. *Progress in Energy and Combustion Science,* 58, pp. 1 – 35.

[43] Wang, H., Zhang, C., Hu, C. & Qi, Y., 2008. Important development trends of coke oven gas utilization in steel plant. *Journal of Iron and Steel Research,* 20(3), pp. 1 – 4.

[44] Kuramochi, T., Ramírez, A., Turkenburg, W. & Faaij, A., 2011. Techno-economic assessment and comparison of CO_2 capture technologies for industrial processes: Preliminary results for the iron and steel sector. *Energy Procedia*, 4, pp. 1981 – 1988.

[45] Hoekman, S. K., & Robbins, C. (2012). Review of the effects of biodiesel on NOx emissions. *Fuel Processing Technology*, 96, pp. 237 – 249.

[46] Vogl, V., Åhman, M. & Nilsson, L. J., 2018. Assessment of hydrogen direct reduction for fossil-free steelmaking. *Journal of Cleaner Production*, 736 - 745, p. 203.

[47] Yilmaz, C., Wendelstorf, J. & Turek, T., 2017. Modeling and simulation of hydrogen injection into a blast furnace to reduce carbon dioxide emissions. *Journal of Cleaner Production*, 154, pp. 488 - 501.

[48] Riley, J., Atallah, C., Siriwardane, R. & Stevens, R., 2021. Technoeconomic analysis for hydrogen and carbon Co-Production via catalytic pyrolysis of methane. *International Journal of Hydrogen Energy*, pp. 1 - 21.

[49] Younas, M., Shafique, S., Hafeez, A., Javed, F., & Rehman, F., 2022. An Overview of Hydrogen Production: Current Status, Potential, and Challenges. *Fuel*, 316, p. 123317.

[50] Johnson, E., 2009. Goodbye to carbon neutral: Getting biomass footprints right. *Environmental Impact Assessment Review*, 29(2), pp. 165 - 168.

[51] Mandova, H., Gale, W. F., Williams, A., Heyes, A. L., Hodgson, P., & Miah, K. H., 2018. Global assessment of biomass suitability for ironmaking – Opportunities for co-location of sustainable biomass, iron and steel production and supportive policies. *Sustainable Energy Technologies and Assessments*, 27, pp. 23 - 39.

[52] Gaster, R. J., Dahotre, N. B. & Hill, R. A., 2003. *Heat Treating and Surface Engineering : Proceedings of the 22nd Heat Treating Society Conference and the 2nd International Surface Engineering Congress.* Materials Park : A S M International.

[53] Alderson, H., Cranston, G. R. & Hammond, G. P., 2012. Carbon and environmental footprinting of low carbon UK electricity futures to 2050. *Energy*, 48(1), pp. 96 - 107.

[54] Yao, X., Yuan, X., Yu, S., & Lei, M. (2021). Economic feasibility analysis of carbon capture technology in steelworks based on system dynamics. *Journal of Cleaner Production*, 322, p. 129046.

[55] Chaczykowski, M., & Osiadacz, A. J. (2012). Dynamic simulation of pipelines containing dense phase/supercritical CO_2-rich mixtures for carbon capture and storage. *International Journal of Greenhouse Gas Control*, 9, pp. 446 - 456.

[56] Kjärstad, J., Skagestad, R., Eldrup, N. H., & Johnsson, F. (2016). Ship transport—A low cost and low risk CO_2 transport option in the Nordic countries. *International Journal of Greenhouse Gas Control*, 54, pp. 168 - 184.

[57] Dugstad, A., Halseid, M., & Morland, B. (2013). Effect of SO_2 and NO_2 on Corrosion and Solid Formation in Dense Phase CO_2 Pipelines. *Energy Procedia*, 37, pp. 2877 - 2887.

[58] Onwuemezie, L., Darabkhani, H. G., & Montazeri-Gh, M. (2024). Pathways for low carbon hydrogen production from integrated hydrocarbon reforming and water electrolysis for oil and gas exporting countries. *Sustainable Energy Technologies and Assessments*, 61, p. 103598.